.

A Study on Performance of Simplified Vehicle Models in Optimization of Hydraulic Engine Mounts in Comparison with Full-Vehicle Model

Y. Rasekhipour[1] and A. Ohadi [2,*]

[1] MSc student, Department of Mechanical Engineering, Amirkabir University of Technology, No. 424, Tehran, IRAN.

[2] Associate Professor, Department of Mechanical Engineering, Amirkabir University of Technology, No. 424, Tehran, IRAN.

* a_r_ohadi@aut.ac.ir

Abstract

Optimization of engine mounts has been investigated in several studies in which different models, a model of a single engine mount to an intricate full-vehicle model, have been used for the optimization. In this paper two simplified vehicle models and a simple full-vehicle model are used in the optimization of the Hyadraulic Engine Mounts (HEMs) to determine whether optimization through the simplified models can result in appropriate HEMs or the simple full-vehicle model or even more intricate models has to be used in the optimization process. Hydraulic Engine Mounts (HEMs) are optimized through a global optimization method called Direceted Tabu Search (DTS) method in order that the best ride comfort is achieved for the vehicle system.

1. INTRODUCTION

The main role of engine mounting system as one of the principal vehicle vibration isolating systems, besides suspension system, is to reduce the Noise, Vibration and Harshness (NVH) perceived by driver and to improve the ride comfort. The main vehicle NVH sources are low frequency road roughness and high frequency engine force. Thus, engine mounts should be capable of adequate isolation in a wide range of frequency. Almost constant stiffness and damping of rubber engine mounts with respect to frequency, leaded vehicle industries to develop Hydraulic Engine Mounts (HEMs). A HEM equipped with inertia track and decoupler performs a desirable performance in a wide range of frequency [1]. The unfavorable high stiffness in fluid resonance frequency motivated the development of bell plate. Equipping the HEM with bell plate provides a good performance in all working frequencies [2]. A better performance will be achieved if an appropriate HEM is provided by executing an optimization process.

Optimization based on modal analysis has been performed in several studies for rubber engine mounts. Arai et al. [3] and Suresh et al. [4] focused on transmitted force to the vehicle body using modal analysis. Liu [5], Sui et al. [6], Akanda and Adulla [7], and Weng [8] sought a better performance through

mode decoupling method. Modal analysis is not useful for nonlinear systems, so it cannot be used for vehicle systems benefiting HEMs. In addition, there is no guarantee that the system designed to decouple modes exhibits the best performance, e.g. the system will have a better ride comfort performance if the optimization objective is ride comfort than if it is to decouple system modes.

All studies on optimization of HEMs have been performed in single HEM system, or a 1DOF-mass mounted on a HEM system. Ahn et al. [9,10] studied a single HEM system and minimized the total force transmissibility in the notch and the resonance frequencies. Li et al. [11] routed to a single HEM system, and optimized the mount such that some of its characteristics, i.e., resonance frequency and dynamic stiffness value at resonance frequency approached to their desired values. Lee et al. [12] investigated a single degree of freedom mass mounted on an active hydraulic engine mount, and optimized the mount by minimizing dynamic stiffness, and maximizing dynamic damping and active force.

Some investigations on rubber mounts have been preceded for engine mounted systems. Yuan et al. [13] determined the best mount among available rubber mounts by optimizing the mounts in an engine system with minimum total transmitted force to the ground as the objective, and selecting the most similar one to the

optimized mount. Several studies on optimization of rubber mounts have been performed in full vehicle systems. Bretl [14] and Wang et al. [15] optimized rubber engine mounts in full vehicle system to minimize the vibration of driver position. Foumani et al. [16] preceded an experimental/numerical technique to improve the accuracy of the model via experiment, and optimized engine mounts in a precise vehicle system with displacement transmissibility from road to the engine as its objective. Madjlesi et al. [17] optimized the rubber mounts in a vehicle system to minimize the vibration of steering wheel. Lee et al. [18,19] focused on the structure-borne noise due to powertrain vibration and minimized the interior noise level over a certain engine rotating-speed range by optimizing rubber engine mounts. Several kinds of systems from a simple single engine mount system to an intricate vehicle system have been investigated in the above mentioned studies; it is not known whether it is required to optimize the engine mounts in an intricate full-vehicle system or the simpler systems are adequate for the optimization.

The system of interest in this study is a vehicle system whose engine is mounted to the chassis via three HEMs. It is desired to improve the ride comfort, and the vertical acceleration of the driver position is used as the ride comfort index. A 13DOF model (Fig. 1(a)) called model No. 1 is used as the reference model of the system. Two simpler models are also investigated. An appropriate simplified model for optimization of the HEMs is a 6DOF engine mounted

to the ground via three HEMs (Fig. 1(b)) called model No. 2. Besides, a simplification in model No. 2 results in a 1DOF body which is mounted to the ground via one HEM (Fig. 1(c)) called model No. 3. Optimization is performed for these three models, and for each model, the optimized parameters of the HEM(s) are obtained. The resulted optimized parameters are used in the reference full vehicle model. The ride comfort indexes of the three resultant reference models are compared to clarify whether optimization in model No. 2 or model No. 3 can result in a favorable performance, or the optimization have to be performed for the model No. 1.

In this study, a global optimization method called Directed Tabu Search (DTS) method is used, which is the result of combining Tabu Search (TS) method with direct search methods [12]. Memory structures are the main elements of a TS method which improve the performance of the method by avoiding searching visited regions. It causes the method to search more regions with equal number of function evaluations that makes DTS advantageous over other global optimization methods.

The structure of the paper is as follows. Initially the mathematical model for each model is obtained. Next, a study on HEM parameters is performed to determine the most effective parameters to be used as design parameters in optimization. Then, DTS method is explained and objective functions and constraints of the optimization are determined. Finally, optimization results are expressed, the corresponding results are
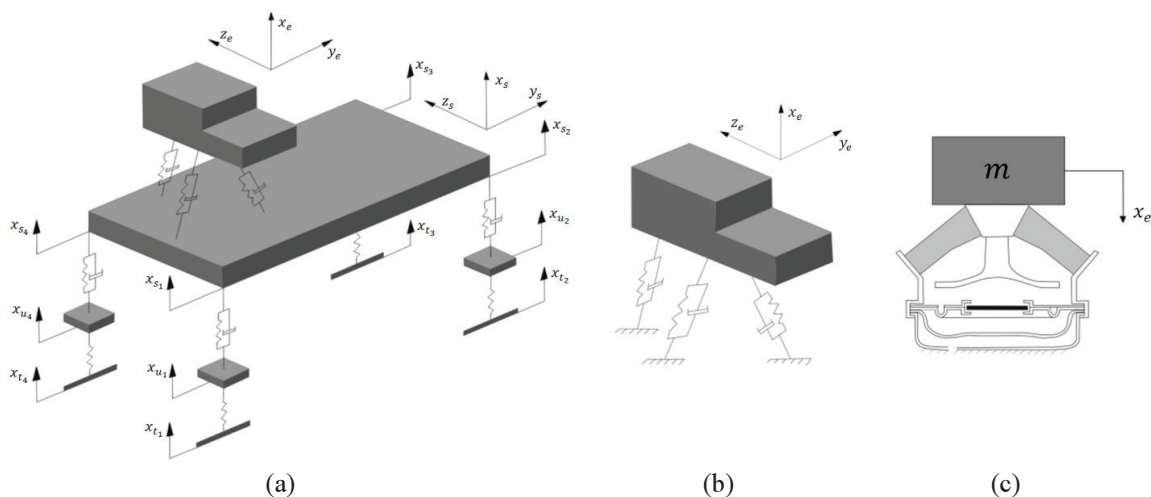

Fig. 1. Optimization models, (a) Model No. 1 - 13 DOF full-vehicle (reference model), (b) Model No. 2 - 6DOF engine mounted to the ground via three HEMs, (c) Model No. 3 - 1DOF engine supported on a HEM.

substituted in the reference model, and comparison between three models is done.

2. MATHEMATICAL MODEL

2. 1. Mathematical Model of HEM

The HEM of interest is structurally similar to the conventional HEM except that a bell plate is added to it. The improvement in the behavior of conventional HEM by supplementing bell plate to it is studied by Ohadi and Fakhari [2]. Cross Section and lumped parameter system model of the HEM are illustrated in Fig. 2 [1]. As demonstrated in Fig. 2(b), the HEM contains three chambers: bell chamber, upper chamber, and lower chamber, and three passages: inertia track, decoupler, and bell plate.

Excitation causes relative motion of the two ends of the HEM; thus pressure varies in the chambers which motivates the fluid to flow through the three passages. The fluid passing the inertia track, which is a long narrow passage, causes a high damping. But in high frequency behavior, low damping is required which motivated the creation of the decoupler [1]. In high frequencies, the decoupler disk, which lies on one of its limits and blocks the decoupler passage in low frequencies, stands in the middle, and the pressure difference between the upper and lower chambers causes the fluid to flow through the decoupler –which is a short wide passage- instead of the inertia track. Undesirable behavior due to resonance of the

containing fluid, which causes high stiffness in fluid resonance frequency, motivated the development of bell plate.

Continuity equations for the three chambers are:

$$C_b \dot{P}_b = Q_b - (A_m - A_b - A_p)\dot{X}_e \tag{1}$$

$$C_1 \dot{P}_1 = (A_m - A_b)\dot{X}_e - Q_b - Q_i - Q_d \tag{2}$$

$$C_2 \dot{P}_2 = Q_i + Q_d \tag{3}$$

in which C_b, C_1 and C_2 are the compliances of bell chamber, upper chamber and lower chamber, respectively. P_b, P_1 and P_2 represent the pressures of bell chamber, upper chamber and lower chamber and Q_b, Q_i and Q_d are the flows passing through bell passage, inertia track and decoupler, respectively. A_b is the area of bell plate, A_p represent effective pumping area, A_m is the area of the HEM, and X_e is the displacement of the upper end of the HEM. Momentum equations for inertia track, decoupler and bell plate, respectively, are:

$$P_1 - P_2 = I_i \dot{Q}_i + (R_i + R_i'|Q_i|)Q_i \tag{4}$$

$$P_1 - P_2 = I_d \dot{Q}_d + (R_d + R_d'|Q_d| + R_0 e^{\left(\frac{X_d}{X_0}\right)\arctan\left(\frac{Q_d}{Q_0}\right)})Q_d \tag{5}$$

$$P_1 - P_b = I_b \dot{Q}_b + (R_b + R_b'|Q_b + A_b\dot{X}_e|)(Q_b + A_b\dot{X}_e) \tag{6}$$

in which I represents the inertia of each passage, R and R' represent the resistances of each passage due to
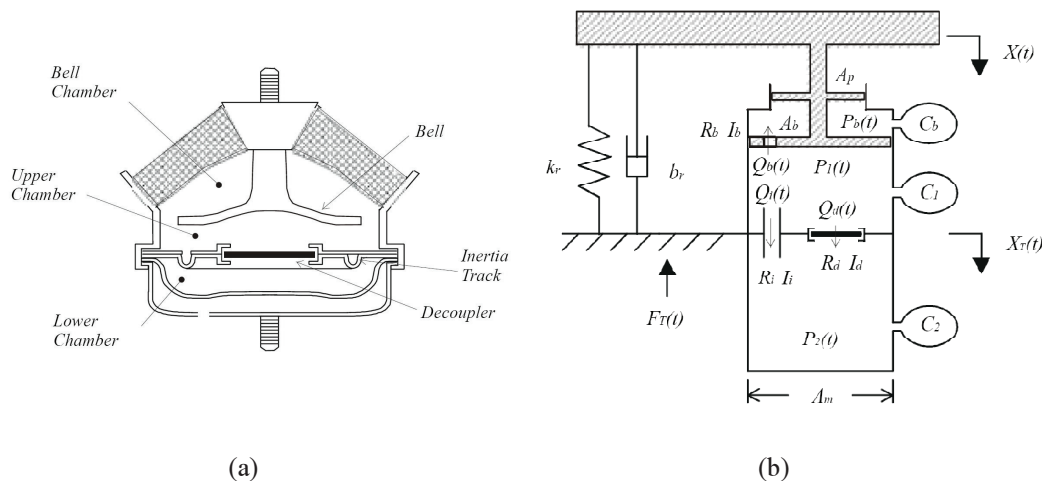

Fig. 2. (a) Cross section of HEM - (b) Lumped parameter system model of HEM [21].

4

A Study on Performance of Simplified Vehicle Models in Optimization ...

laminar flow and turbulent flow, and i, d and b indices represent the inertia track, decoupler, and bell passage. First, second and third terms on the right side of Eqs. 4-6 demonstrate momentum resulting by fluid inertia, resistance due to laminar flow, and resistance due to turbulent flow, respectively. The last terms on the right side of Eq. 5 represents the additional resistance created by decoupler disk when it approaches any of its limits [1].

Transmitted force to the base of the HEM, F_T is:

$$F_T = C_r \dot{X}_e + K_r X_e + (A_m - A_{d-fnc})(P_1 - P_2) + A_m P_2$$
$$+ A_d (R_d + R'_d |Q_d|) Q_d - (A_m - A_p) P_b \quad (7)$$

in which K_r and C_r are the stiffness and damping of rubber part of the mount, respectively, and $A_{d\text{-}fnc}$ is the equivalent decoupler area defined in order to express the transmitted force in a continuous equation for both occasions when the decoupler disk blocks the passage and when it does not [1]:

$$A_{d-fnc} = \frac{1}{\pi} A_d \left[\frac{\pi}{2} - \arctan \left(\frac{\left(\frac{2}{\pi} \right) X_d \arctan \left(\frac{P_1 - P_2}{P_0} \right) - X_{d-max}}{X_1} \right) \right] \quad (8)$$

Moreover, the force acting on the upper end of the HEM differs from the transmitted force to the base:

$$F = C_r \dot{X}_e + K_r X_e + (A_m - A_b) P_1 + \left(A_p - (A_m - A_b) \right) P_b \quad (9)$$

Equations acting on model No. 3 (Fig. 1(c)) are the same as Eqs. 1-9 except that because of the mass placed on the upper end of the mount, Eq. 9 changes to:

$$F = m \ddot{X}_e + K_r X_e + C_r \dot{X}_e + (A_m - A_b) P_1 + \left(A_p - (A_m - A_b) \right) P_b \quad (10)$$

In which F is the excitation force exerted to the mass.

2. 2. Mathematical Model of Vehicle

Reference model of vehicle investigated in this study consists of an engine body mounted to vehicle body, and four wheel bodies jointed to the vehicle body via suspension system, as demonstrated in Fig. 1(a). In this system, engine is modeled as a 6DOF rigid body, mounting to the vehicle body via three similar inclined HEMs. The engine roll axis can

coincide with mount elastic axis, if HEMs lie in an appropriate inclined manner, which decouples roll engine mode from other engine modes, and reduces vibration amplitude [5]. Vehicle body and chassis are modeled as a unified body capable to move in bounce, roll and pitch modes. Four wheels are connected to it via suspension system; each is assumed as a rigid body travels in vertical direction and is connected to the ground through the tire. Suspension system and tires are modeled as linear springs and dampers.

A V-shape four-cylinder engine is studied whose engine force arises from the motion of engine inner bodies including piston, conrod, crankshaft, and balancing system. The engine force acting on the engine body is the only source of excitation. The forces and torques acting on the engine can be expressed in the format [2]:

$$F_E : T_E = a_1 \omega^2 \sin \omega t + a_2 \omega^2 \cos \omega t + a_3 \omega^2 \cos 2\omega t \quad (11)$$

in which a_i i=1,2,3 are determined for each torque or force component. Newton's second law results in the following equations for the wheels:

$$M_{ui} \ddot{x}_{ui} = k_{si} (x_s + z_{si} \theta_{sy} - y_{si} \theta_{sz} - x_{ui}) +$$
$$c_{si} (\dot{x}_s + z_{si} \dot{\theta}_{sy} - y_{si} \dot{\theta}_{sz} - \dot{x}_{ui}) - k_{ti}(x_{ui} - x_{ti}) \quad i = 1, \dots, 4 \quad (12)$$

in which M_{ui} and x_{ui} represent i-th unsprung mass and its vertical displacement, respectively, k_{si} and c_{si} are i-th suspension stiffness and damping, respectively, k_{ti} indicates the i-th tire stiffness, x_s, θ_{sy} and θ_{sz} are bounce, roll, and pitch motions of vehicle body, respectively, x_{ti} is the vertical displacement of the lower end of the tire that represents the road disturbance and is assumed to be zero in this study. Also, y_{si} and z_{si} represent the position of each suspension from vehicle coordinate located on the center of mass of vehicle body. Vehicle body motion originates from the forces transmitted from suspension system and mounting system:

$$M_s \ddot{x}_s = \sum_{i=1}^{3} F_{msxi} + \sum_{i=1}^{4} F_{sxi} \quad (13)$$

$$I_{sy} \ddot{\theta}_{sy} = \sum_{i=1}^{3} (F_{msxi} z'_{mi} - F_{mszi} x'_{mi}) + \sum_{i=1}^{4} F_{sxi} z_{si} \quad (14)$$

$$I_{sz} \ddot{\theta}_{sz} = \sum_{i=1}^{3} (F_{msyi} x'_{mi} - F_{msxi} y'_{mi}) + \sum_{i=1}^{4} (-F_{sxi} y_{si}) \quad (15)$$

in which M_s, I_{sy} and I_{sz} are the mass of the vehicle body and momentum of inertia of it in y- and z-directions, respectively, x'_{mi}, y'_{mi} and z'_{mi} represent the position of each mount in vehicle body coordinate, and F_{sxi} is the force transmitted to vehicle body from suspension system:

$$F_{sxi} = -k_{si}(x_s + z_{si}\theta_{sy} - y_{si}\theta_{sz} - x_{ui}) - c_{si}(\dot{x}_s + z_{si}\dot{\theta}_{sy} - y_{si}\dot{\theta}_{sz} - \dot{x}_{ui}) \tag{16}$$

Inclined HEMs lie in x-y plane, and are oriented at angle α_{mi} related to y-axis. Therefore, F_{msi}, which is the force transmitted from engine mounts, can be formulated as follows:

$$F_{msxi} = (k_{mxi}X_{ei} + c_{mxi}\dot{X}_{ei}) + \Big((A_{pi} - A_{d-fnci})(P_{1i} - P_{2i}) + A_{pi}P_{2i} + A_{di}(R_{di} + R'_{di}|Q_{di}|)Q_{di}\Big)\sin\alpha_{mi} \tag{17}$$

$$X_{ei} = (x_e + z_{mi}\theta_{ey} - y_{mi}\theta_{ez}) - (x_s + z'_{mi}\theta_{sy} - y'_{mi}\theta_{sz}) \tag{18}$$

$$F_{msyi} = (k_{myi}Y_{ei} + c_{myi}\dot{Y}_{ei}) + \Big((A_{pi} - A_{d-fnci})(P_{1i} - P_{2i}) + A_{pi}P_{2i} + A_{di}(R_{di} + R'_{di}|Q_{di}|)Q_{di}\Big)\cos\alpha_{mi} \tag{19}$$

$$Y_{ei} = (y_e + x_{mi}\theta_{ez} - z_{mi}\theta_{ex}) - x'_{mi}\theta_{sz} \tag{20}$$

$$F_{mszi} = k_{mzi}Z_{ei} + c_{mzi}\dot{Z}_{ei} \tag{21}$$

$$Z_{ei} = (z_e + y_{mi}\theta_{ex} - x_{mi}\theta_{ey}) + x'_{mi}\theta_{sy} \tag{22}$$

in which k_{mxi}, k_{myi}, k_{mzi}, c_{mxi}, c_{myi} and c_{mzi} represent the stiffness and damping of each mount in x-, y- and z-direction, respectively, X_{ei}, Y_{ei} and Z_{ei} are the relative displacement of each mount in each direction, x_e, y_e, z_e, $\dot{e}_{ex}$, $\dot{e}_{ey}$ and $\dot{e}_{ez}$ are the displacement and rotation of engine body in each direction, and x_{mi}, y_{mi}, and z_{mi} represent the position of each mount in engine body coordinate, which is located on center of mass of engine body. Engine body motion is caused by force transmitted from engine mounts (F_{mei}) and engine excitation force (F_E, T_E):

$$M_e\ddot{x}_e = -\sum_{i=1}^{3}F_{mexi} + F_{Ex} \tag{23}$$

$$M_e\ddot{y}_e = -\sum_{i=1}^{3}F_{meyi} + F_{Ey} \tag{24}$$

$$M_e\ddot{z}_e = -\sum_{i=1}^{3}F_{mezi} + F_{Ez} \tag{25}$$

$$I_{ex}\ddot{\theta}_{ex} = (I_{ey} - I_{ez})\dot{\theta}_{ey}\dot{\theta}_{ez} - \sum_{i=1}^{3}(F_{mezi}y_{mi} - F_{meyi}z_{mi}) + T_{Ex} \tag{26}$$

$$I_{ey}\ddot{\theta}_{ey} = (I_{ez} - I_{ex})\dot{\theta}_{ez}\dot{\theta}_{ex} - \sum_{i=1}^{3}(F_{mexi}z_{mi} - F_{mezi}x_{mi}) + T_{Ey} \tag{27}$$

$$I_{ez}\ddot{\theta}_{ez} = (I_{ex} - I_{ey})\dot{\theta}_{ex}\dot{\theta}_{ey} - \sum_{i=1}^{3}(F_{meyi}x_{mi} - F_{mexi}y_{mi}) + T_{Ez} \tag{28}$$

in which M_e, I_{ex}, I_{ey}, and I_{ez} are the mass of the engine body and momentum of inertia of it in each direction. As mentioned in the previous section, the force transmitted from the mount to the vehicle body (F_{msi}) is different from the force exerted to the mount by engine (F_{mei}):

$$F_{mexi} = -(k_{mxi}X_{ei} + c_{mxi}\dot{X}_{ei}) + \Big((A_m - A_b)P_{1i} + \big(A_p - (A_m - A_b)\big)P_{bi}\Big)\sin\alpha_{mi} \tag{29}$$

$$F_{meyi} = -(k_{myi}Y_{ei} + c_{myi}\dot{Y}_{ei}) + \Big((A_m - A_b)P_{1i} + \big(A_p - (A_m - A_b)\big)P_{bi}\Big)\cos\alpha_{mi} \tag{30}$$

$$F_{mezi} = -(k_{mzi}Z_{ei} + c_{mzi}\dot{Z}_{ei}) \tag{31}$$

The equations acting on model No. 2 (Fig. 1(b)) can be achieved from Eqs. 23-31 while the displacements and rotations of the vehicle body in Eqs. 18, 20 and 22 are zero.

3. PARAMETER STUDY

In an optimization process, first of all, design parameters which are the most effective parameters, must be specified. In this study, it is desired to optimize HEMs in order to improve the vibration behavior of vehicle. Thus, a parameter study is
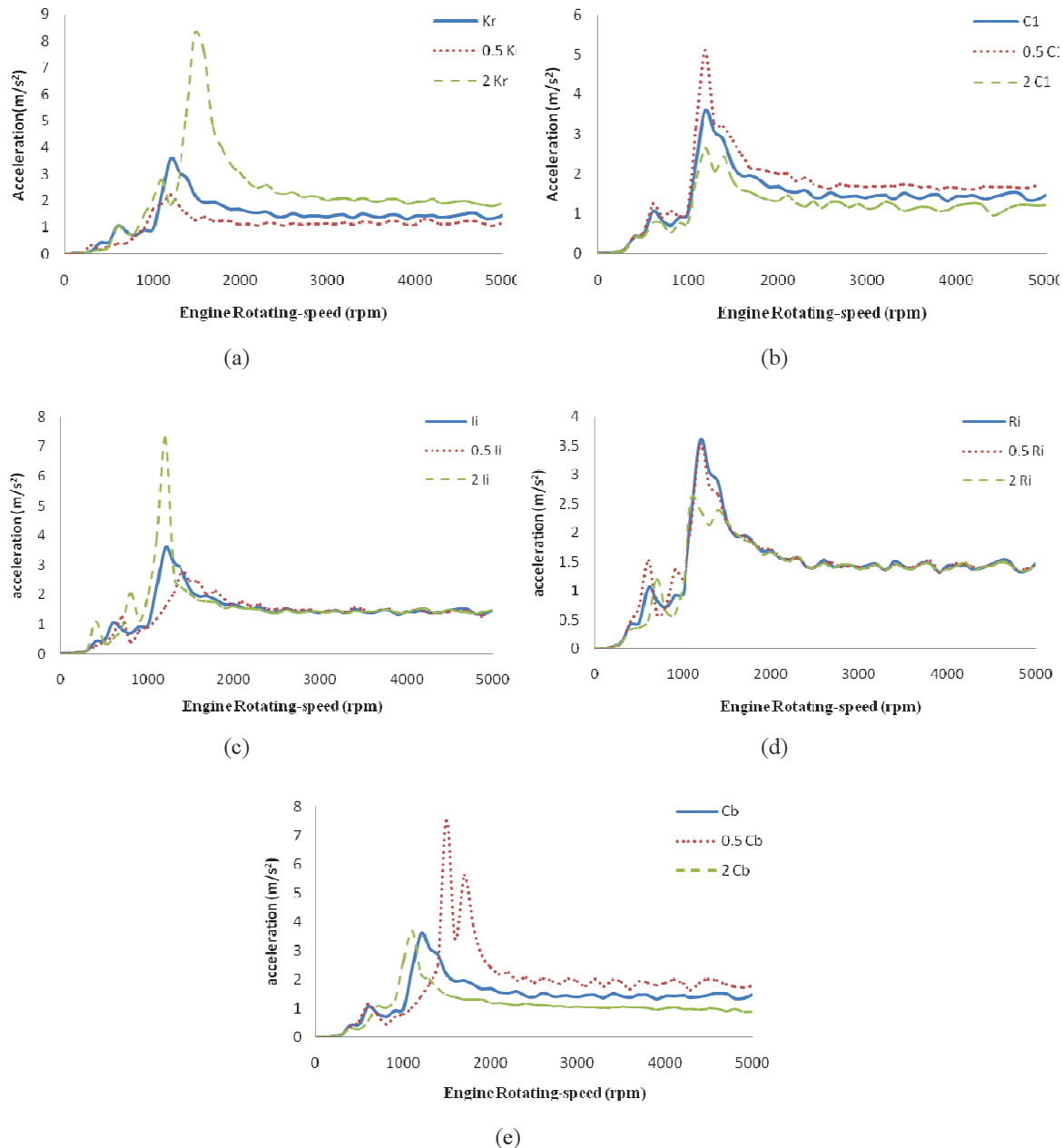
(a)

(b)

(c)

(d)

(e)

Fig. 3. Effect of design parameters on driver position acceleration: (a) rubber stiffness, (b) upper chamber compliance, (c) inertia of inertia track, (d) resistance of inertia track, and (e) bell chamber compliance

performed to determine the most effective parameters of the HEM on vibration behavior of vehicle.

Several researchers have investigated the design parameters through sensitivity analysis [3, 4]. This paper goes through a direct way to do so. The procedure is performed by varying each parameter while others remain unchanged, and plotting vibration behavior of the system for three different amounts of the parameter [6] (the original value, half of it, and

double of it). The plots clearly illustrates how the vibration behavior alters as each parameter changes; so, by studying all changeable parameters of the HEM and a brief look at the plots, the most effective parameter can be specified.

HEM parameters including K_r, C_r, C_1, C_2, I_i, R_i, I_d, R_d, C_b, I_b, R_b and A_b are studied to determine the design parameters. Fig. 3 shows the influence of the most effective parameters on driver position

acceleration in the range of 0-5000 rpm of engine rotating speed (Values of HEM parameters and vehicle parameters used in the simulation are presented in appendix A and B, respectively). For each value of parameters, the simulation is performed for different amounts of engine rotating speed, and the peak value of the driver position acceleration at steady state condition is determined to construct the plots. It is clear from the figures that these parameters have a great influence on vibration behavior of the system. Thus, design parameters are chosen to be K_r, C_1, I_i, R_i and C_b.

4. OPTIMIZATION PROCESS

4. 1. Optimization Method

The optimization method executing in this study is Directed Tabu Search (DTS) method being a developed version of Tabu Search (TS) method. TS is an optimization method benefiting memory elements to avoid searching visited regions, and DTS is the result of combining TS with some direct search methods such as Adaptive Pattern Search (APS) method. DTS is a global optimization method which performs local search from plenty of initial points instead of one, in which the best point among the resultant local optimized points is the global optimized point.

Three search procedures are used in DTS: Exploration, Diversification, and Intensification. In the exploration search, local search is performed by employing APS strategy to lead the search, and introducing memory elements called Tabu List (TL), Tabu Regions (TRs), and Semi-TRs to prevent cycling. The diversification search generates new trial points to be used as initial points of the exploration search. It benefits another memory element called Visited Regions List (VRL) to diversify the search from the visited points. Eventually, the intensification search performs local searches from the best points arisen from previous search procedures, to intensify the answer.

The main loop of DTS consists of exploration and diversification searches. It starts from an initial point x_0, and exploration procedure starts from this initial point in a loop called inner loop. After the inner loop is accomplished, diversification search generates another point to be used as initial point of the inner

loop in the next main loop iteration.

In the exploration search, memory elements including TL, TRs, and Semi-TRs are introduced to prevent searching in neighborhood of the best points and recently visited points in order to avoid cycling and search a broader area. Each resultant point of the exploration process is ranked in ascending order by both its recency and its objective function value to be stored in TL. Since definite quantity of points are stored in TL, just the most recent points and the best points are stored. TRs are defined to be regions around each point of TL with radius r_{TR}, and Semi-TRs are defined to be surrounding regions around TRs with radius $r_{STR} > r_{TR}$. Thus, if the trial points do not enter TRs, exploration search has avoided cycling. So, if the current point is in Semi-TRs, the direction of generating trial points will be outward from the center of Semi-TRs and the step size of generating new trial points along each axis will be chosen much greater than TR radius. Otherwise trial points are generated in a random direction along each axis. In the both above mentioned procedures, if one of the trial points is better than the current point, it is chosen as the resultant point and this iteration of the inner loop is accomplished, otherwise local points are generated employing APS and the best point among these local points and trial points is chosen as the resultant point of this inner loop iteration. Simply said, TL, TRs, and Semi-TRs exclude the visited regions from the search area, and the search is directed to the local optimized point by APS, instead of using a random search performed in conventional TS. The resultant point is added to TL and VRL, and is used as initial point for the next inner loop iteration.

The inner loop is terminated if it cannot achieve improvement in l'_{inner} iterations, or l_{inner} iterations are performed. After the inner loop is terminated, diversification search is executed. It introduces a memory element called VRL to diversify the search. VRL is defined to be a spherical region around each resultant point. The center of sphere as well as frequency of visiting the point is stored in VRL. In the diversification search, a random trial point is generated and is checked whether it is in neighborhood of any visited region. A function determines if the point or its neighborhood has been visited and the frequency of being visited. According to the function value, if the neighborhood of the generated point has not been visited, the

diversification is accomplished; otherwise a new trial point is generated and is checked. If the procedure is unsuccessful for specified times, the point with less frequency of being visited will be chosen by means of the function. The resulting point will be the initial point for inner loop in the next main loop iteration. The main loop is terminated if it cannot achieve improvement in l'_{main} iteration, or l_{main} iterations are performed.

Assuming that the procedure has searched the entire optimization region, the best points of TL can make the best local optimized points if the intensification search is performed for them. Thus, in the intensification search, some local optimization processes are performed whose initial values are the best points of TL. The best point among the local optimized points is the global optimized point.

4. 2. Objective Function

One of the main indexes of an appropriate vehicle is its ride comfort. In this study the vertical acceleration of the driver position is chosen as the ride comfort index, and the objective of this study is to reduce it. HEM in the three models is optimized and the resultant HEMs of each model are replaced the original HEM in the reference model. Ride comfort index of the three resultant reference models are evaluated to determine whether simplified models are capable to optimize the HEMs for vehicle or optimization is required to be executed for more intricate models. The objective of model No. 1 is minimizing the driver position acceleration. For the two other models, the objective has to be chosen such that the resultant HEMs can afford the objective of the reference model (which is identical with model No. 1). Since transmitted force to the chassis is the source of vibration of the chassis, the objective of the two models No. 2 and 3 is selected to be the transmitted force to the ground. In all three models, the objective function is the least mean squares of the mentioned objectives in the frequency range of 0-200Hz. Besides, the excitation of the system has to be modeled appropriately so that the optimization results in proper HEMs for the vehicle. For models No. 1and 2 it is the engine force acting on engine [2], and for model No. 3 it is chosen to be one third of vertical component of engine force acting on the mounted mass. The engine rotating speed (the frequency of the

excitation force) sweeps in time from 1000 to 5000 rpm in the simulation of the models.

The designer cannot assign any desired amount to the design parameters. So, before the optimization procedure is started, constraints, which must be held on them, have to be specified. As the length and area of the inertia track can vary independently, I_i and R_i can alter independently; but the length and the area cannot get any amount, so I_i and R_i should have limits. C_1 and C_b can alter by changing the chambers walls materials. It can be done by adding soft materials to the walls or harden the walls. Similarly, they cannot take any value, because of the limitations in materials. These four parameters can vary in the range of half of their original value to double of it in the optimization. The duty of bearing the engine weight is one of the engine mount tasks that the rubber part of the HEM carry it out. Moreover, lowering the rubber stiffness may shorten its fatigue life and make it lower than the desired value. Thus the lower limit of the stiffness is chosen to be the original value, and the upper limit to be double of it. The design parameters used in DTS are the ratio of the design parameter to their original values:

$$0.5 \leq K_r \leq 2, \qquad 0.5 \leq C_1 \leq 2, \qquad 0.5 \leq I_i \leq 2,$$
$$0.5 \leq R_i \leq 2, \qquad 0.5 \leq C_b \leq 2 \qquad (32)$$

5. RESULTS

In this study, it is desired to determine whether it is required to precede the optimization for an intricate model of vehicle to achieve desired ride comfort performance or it is enough to optimize the HEMs in a simple model. A 13DOF model is used as the reference model (model No. 1), and is simplified twice to constitute two other models (Fig. 1). A procedure is performed for each of the three models; the optimized HEMs of the model is obtained via DTS, and the original HEMs in the reference model are replaced by this HEMs to create three resultant reference models, then vertical acceleration of the driver position- as the ride comfort index- of each resultant reference model is evaluated to determine which model is more appropriate to be used for optimization.

Optimization results for the three models are expressed in table 1. Since model No. 1 is the reference model, its global optimized point is chosen as the reference to evaluate the optimization result of

the two other models. For each of the two simplified models, five of the best points resulted from optimization are chosen and shown in this table. These points are selected such that the distance between every two of the five points is at least 0.2 in order that five local optimized points from five distinct regions are evaluated. The distance between every two points can be calculated as follows:

$$d = \sqrt{\left(K_{r_1} - K_{r_2}\right)^2 + \left(C_{1_1} - C_{1_2}\right)^2 + \left(I_{i_1} - I_{i_2}\right)^2 +}$$

$$\overline{\left(R_{i_1} - R_{i_2}\right)^2 + \left(C_{b_1} - C_{b_2}\right)^2} < 0.2 \qquad (33)$$

Since the design parameters are nondimensional, they can be added to each other. DTS makes it possible to select best points from distinct regions, since it searches all the design area for local optimized points and provides the best points in every region while other global optimization methods do not obtain the best points of each region.

Since the simplified models are structurally different from the full vehicle system, and acceleration and force (the objectives of the reference model and simplified models, respectively) are different in nature, the global optimized point of the simplified models do not coincide the global optimized point of the reference model, and even may exhibit an undesirable response in reference model. But if all the best points of a simplified model exhibit a desirable response in resultant system (resulting from replacing the original HEMs of the reference model by optimized HEMs), it will be concluded that the optimization of the simplified model robustly

performs well, and the simplified model can be used safely instead of the reference model in the optimization process. Thus the average of the five best points of each simplified system, tabulated in table 1, is used as the index of effectiveness of the optimization of the simplified model.

The last two columns of the table, for each point, indicate the percentage of improvement in the objective function of the applied model, and the percentage of improvement in the objective function of the resultant reference model. All percent values are determined with respect to the original values of objective functions. Moreover, the first column indicates whether the point is global optimized point (G) or local optimized one (L).

Table 1 shows 71.09% improvement resulting from optimization of the reference model demonstrating that the optimization is necessary for the system. Besides, global optimized point of model No. 2 results in 67.74% improvement in the behavior of the resultant reference model; and the average of the improvement due to the five best points resulted from optimization of the model is 68.0%. This demonstrates that a small variation in the system parameters may result in another optimal point which will perform similar to the current optimal point i.e. the optimization is robust. It is noticeable that the point L#3 makes a more improvement in the resultant model in comparison with global optimized point, which is because of the different structures of reference model and model No. 2. The similar observation for model No. 3 shows that its global optimized point performs 66.72% improvement in the behavior of the resultant
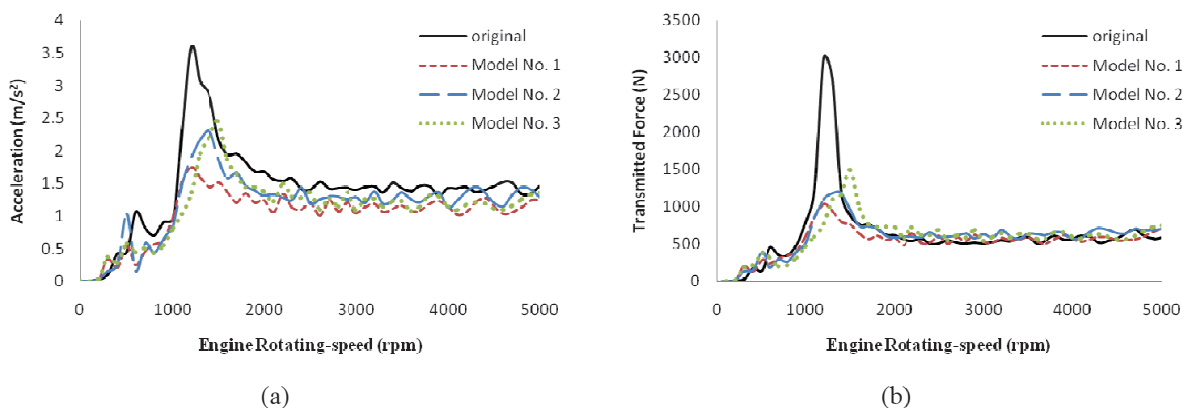
Fig. 4. Optimized systems in comparison with original system: (a) acceleration of driver position, (b) transmitted force from engine body.

Table 1. Optimization results for the three models

Global or Local optimized point	Optimized parameters					improvement in optimized model (%)	improvement in resultant reference model (%)
	K_r	C_1	I_i	R_i	C_b		
Model No. 1							
G	0.5147	1.3900	0.6824	1.6095	0.8466	71.0939	71.0939
Model No. 2							
G	0.5743	1.1449	0.7750	1.5687	0.7713	40.0748	67.7381
L #1	0.5639	0.8569	0.8478	1.9416	0.6912	39.5395	67.2012
L #2	0.5861	0.6563	0.8123	1.6212	0.7896	38.8885	66.1268
L #3	0.5411	0.9092	0.7617	1.5393	0.7039	38.2942	69.5650
L #4	0.5433	0.6511	0.7874	1.4376	0.7714	38.0797	69.1943
							ave=67.9651
Model No. 3							
G	0.5184	1.4105	0.6873	0.9174	0.7223	75.3843	66.7239
L #1	0.5006	0.8275	0.7651	0.9474	0.5695	74.8317	64.0848
L #2	0.5965	1.4112	0.5569	0.926	0.7044	73.0816	60.3241
L #3	0.5963	1.0904	0.557	0.9263	0.7047	72.8746	60.1405
L #4	0.5239	0.671	0.5229	0.7296	0.5171	72.6557	59.0675
							ave=62.0682

reference model, and the best five optimal points of the system exhibit an average improvement of 62.1%.

Obtained results indicate that, for the optimization, the reference model (model No. 1) can be replaced by model No. 2 with an insignificant loss of about 3% of improvement. Moreover, if model No. 3 is used for the optimization, an average loss of 9% will be occurred in improvement of the system, which is also acceptable. The loss is because of the different structures of model No. 3 and the reference model; but since the mass is chosen one third of the engine mass and the excitation force is selected to be one third of the vertical component of the engine force in model No. 3, the model can somehow simulate the behavior of the intricate reference model and the results are somehow acceptable.

The vibration behavior of the reference model resulting from global optimized point of each model is compared to the original reference model in Fig. 4. Both plots demonstrate the improved behavior of the system due to optimization of each model. But it can be noticed from the plots that though the objective functions of the resultant reference model of global optimizad points of the three models are so close (as table 1 demonstrates), their maximum values of the driver position acceleration and transmitted force to the chassis are widely different. It indicates that different objective functions result in different global

optimized points, e.g. if the maximum value of the driver position acceleration in a range of engine rotating-speed is used as the objective function, the optimized points will be different.

6. CONCLUSION

Ride comfort of a vehicle is desired to be improved by optimization of its HEMs in this study. A full-vehicle model (model No. 1) is a highly nonlinear model with many degrees of freedom, and if its engine is mounted by HEMs, its nonlinearity makes the simulation more intricate; so if a simplified model like an engine mounted to the ground (model No. 2), which only contains the degrees of freedom of the engine and nonlinearity of its HEMs, or a 1DOF body mounted to ground by a HEM (model No. 3) can afford the optimization and result in an acceptable performance, the optimization is preferred to be done for these simplified models.

Different structures of the models make the optimal region of the reference model different from those of the simplified models. However, if the optimal regions of a simplified model coincide with not the best but appropriate enough regions of the reference model i.e. best local optimized points of the simplified model result in good enough behavior of resultant reference model, the optimization can be done for the simplified

model instead of the reference model. The obtained results indicate that both simplified models exhibit a good performance, and can be used for optimization process instead of full-vehicle model. Model No. 2 shows an insignificant loss of 3% in improvement of optimization if it is used instead of the reference model, which makes it completely reasonable to be preferred for the optimization. Besides, model No. 3 causes a loss of 9% in the improvement of the optimization if it is used for the optimization instead of the reference model. Thus, it is rational to use model No. 3 for the optimization except that the optimization improvement is more important than optimization cost, in which case model No. 2 is to be used. As a conclusion, instead of the complex full-vehicle model which is too hard to be thoroughly modeled, a model of a 1DOF body mounted on the ground via one HEM can be used.

REFERENCES

[1] A. Geisberger, A. Khajepour, F. Golnaraghi, "Non-linear Modeling of Hydraulic Mounts: Theory and Experiment," Journal of Sound and vibration (2002) 249(2), 371-397

[2] A. R. Ohadi, V. Fakhari, "Effect of Bell Plate on Vibration Behavior of Automotive Engine Supported by Hydraulic Engine Mounts," SAE Technical Paper Series 07NVC-223

[3] T. Arai, T. Kubozuka, S. D. Gray, "Development of an Engine Mount Optimization Method Using Modal Parameters," SAE Technical Paper Series 932898

[4] N. Suresh, S. Shankar, N. Manohar, "Optimum Design of Engine and Body Mounts at Total System Level Using Unconstrained Minimization," SAE Technical Paper Series 950584

[5] C. Q. Liu, "A Computerized Optimization Method of Engine Mounting System," SAE Technical Paper Series 2003-01-1461

[6] J. S. Sui, C. Hoppe, J. Hirshey, "Powertrain Mounting Design Principles to Achieve Optimum Vibration Isolation with Demonstration Tools," SAE Technical Paper Series 2003-01-1476

[7] A. Akanda, C. Adulla, "Engine Mount Tuning for Optimal Idle and Road Shake Response of Rear-Wheel-Drive Vehicles," SAE Technical Paper Series 2005-01-2528

[8] J. Weng, "Robust Optimization Design of the Power-train Mounting System of the Light Truck," SAE Technical Paper Series 2007-01-0556

[9] Y. K. Ahn, J. D. Song, B. S. Yang, "Optimal Design of Engine Mount Using an Artificial Life Algorithm," Journal of Sound and Vibration 261 (2003) 309–328

[10] Y. K. Ahn, J. D. Song, B. S. Yang, K. K. Ahn, S. Morishita, "Optimal Design of Nonlinear Hydraulic Engine Mount," Journal of Mechanical Science and Technology (KSME Int J), Vol 19. No 3, pp. 768~777, 2005

[11] Q. Li, J. C. Zhao, B. Zhao, X. S. Zhu, "Parameter Optimization of a Hydraulic Engine Mount Based on a Genetic Neural Network," Proc. IMechE Vol. 223 Part D: J. Automobile Engineering, 2009

[12] B. H. Lee, C. W. Lee, "Optimal Design of Electromagnetic Type Active Control Engine Mount in Consideration of Actuator Efficiency," SAE Technical Paper Series 2007-01-2424

[13] W. Yuan, X. Wang, S. Han, "Optimal Mount Selection with Scattered and Bundled Stiffness Rates," SAE Technical Paper Series 2006-01-0736

[14] J. Bretl, "Optimization of Engine Mounting Systems to Minimize Vehicle Vibration," SAE Technical Paper Series 931322

[15] T. Wang, F. Sturla, V. C. Salazar, "Mount Rate Robust Optimization for Idle Shake Performance," SAE Technical Paper Series 2004-01-1536

[16] M. S. Foumani, A. Khajepour, "Optimisation of Engine Mount Characteristics Using Experimental/Numerical Analysis," Journal of Vibration and Control, 9: 1121–1139, 2003

[17] R. Madjlesi, A. Khajepaour, F. Ismail, J. Mihalic, B. Rice, "Advance Noise Path Analysis, A Robust Engine Mount Optimization Tool," SAE Technical Paper Series 2003-01-3117

[18] K. K. Choi, W. Duan, "Design Sensitivity Analysis and Shape Optimization of Structural Components with Hyperelastic Material," Computer Methods in Applied Mechanics and

Engineering, 187 (2000) 219-243

[19] D. H. Lee, W. S. Hwang, "Parametric Optimization of Complex Systems Using a Multi-domain FRF-based Substructuring Method," Computers and Structures 81 (2003) 2249–2257

[20] A. R. Hedar, M. Fukushima, "Tabu Search Directed by Direct Search Methods for Nonlinear Global Optimization," European Journal of Operational Research 170 (2006) 329–349

[21] A. A. Geisberger, "Hydraulic Engine Mount Modeling, Parameter Identification and Experimental Validation" Thesis for Master of Applied Science in Mechanical Engineering, University of waterloo (2000)

Nomenclature

A_b annular bell area

A_d Decoupler area

$A_{(d-fnc)}$ function for nonlinear decoupler area

A_m area of mount at the bell

A_p effective pumping area of the upper compliance

C_b compliance of the bell chamber

$c_{mxi}, c_{myi}, c_{mzi}$ Damping coefficient of rubber part of each inclined HEM in x-, y-, and z-direction

C_r damping coefficient of the rubber part

c_{si} damping coefficient of each suspension

C_1 compliance of the upper chamber

C_2 compliance of the lower chamber

F transmitted force to mount base

F_E, T_E engine excitation force and torque

F_{mei} force transmitted from each engine mount to engine body

F_{msi} force transmitted from each engine mount to vehicle body

F_{sxi} force transmitted to vehicle body from each suspension

I_b fluid inertia of the bell

I_d fluid inertia of the decouple

I_{ex}, I_{ey}, I_{ez} momentum of inertia of engine body in x-, y-, and z-direction

I_i fluid inertia of the inertia track

I_{sy}, I_{sz} momentum of inertia of vehicle body in y- and z-direction

$k_{mxi}, k_{myi}, k_{mzi}$ stiffness of rubber part of each inclined HEM in x-, y-, and z-direction

K_r stiffness of the rubber part

k_{si} stiffness of each suspension

k_{ti} stiffness of each tire

M_e mass of the engine body

M_s Mass of vehicle body

M_{ui} mass of each unsprung body

P_b pressure in the bell chamber

P_1 pressure in the upper chamber

P_2 pressure in the lower chamber

Q_b flow through the bell

Q_d flow through the decoupler

Q_i flow through the inertia track

R_b fluid flow resistance across the bell

R_b' fluid resistance parameter on squared flow across the bell

R_d fluid flow resistance across the decoupler

R_d' fluid resistance parameter on squared flow across the decoupler

R_i fluid flow resistance across the inertia track

R_i' fluid resistance parameter on squared flow across the inertia track

x_e, y_e, z_e displacement of engine body in x-, y-, and z-direction

X_{ei}, Y_{ei}, Z_{ei} relative displacement of each mount in x-, y-, and z-direction

x_{mi}, y_{mi}, z_{mi} position of each mount in engine body coordinate in x-, y-, and z-direction

$x'_{mi}, y'_{mi}, z'_{mi}$ position of each HEM in vehicle body coordinate in x-, y-, and z-direction

x_s bounce motion of vehicle body

x_{ti} road disturbances

x_{ui} vertical displacement of each unsprung body

y_{si}, z_{si} position of each suspension in y- and z-direction

α_{mi} angle of each inclined HEM related to y-axis

$\theta_{ex}, \theta_{ey}, \theta_{ez}$ rotation of engine body in x-, y-, and z-direction

θ_{sy} roll motion of vehicle body

θ_{sz} pitch motion of vehicle body

Appendix A: HEM Parameters Values

Table 2. HEM parameters

Parameter	Amount	Parameter	Amount	Parameter	Amount	Parameter	Amount
$A_p (m^2)$	2.5e-3	$R'_d \left(\frac{kg}{m^7}\right)$	4.25e10	$Q_0 \left(\frac{m^3}{s}\right)$	1e-14	$C_{mz} \left(\frac{N\,s}{m}\right)$	20
$A_b (m^2)$	6e-4	$I_b \left(\frac{kg}{m^4}\right)$	2e4	$K_r \left(\frac{N}{m}\right)$	2.25e5	$x_{m1} (m)$	-0.2311
$A_m (m^2)$	4.9e-3	$R_b \left(\frac{kg}{s\,m^4}\right)$	2.8e5	$C_r \left(\frac{N\,s}{m}\right)$	100	$x_{m2} (m)$	0.1052
$C_1 \left(\frac{m^5}{N}\right)$	7e-13	$R'_b \left(\frac{kg}{m^7}\right)$	2.97e9	$\alpha_{m1} (°)$	83	$x_{m3} (m)$	0.0149
$C_2 \left(\frac{m^5}{N}\right)$	2.6e-9	$X_{d-max} (m)$	5.3e-4	$\alpha_{m2} (°)$	90	$y_{m1} (m)$	-0.3183
$C_b \left(\frac{m^5}{N}\right)$	3e-11	$X_0 (m)$	3.15e-5	$\alpha_{m3} (°)$	97	$y_{m2} (m)$	-0.0038
$I_i \left(\frac{kg}{m^4}\right)$	3.8e6	$R_0 \left(\frac{kg}{s\,m^4}\right)$	1e-4	$k_{mx} \left(\frac{N}{m}\right)$	2.23e5	$y_{m3} (m)$	0.0914
$R_i \left(\frac{kg}{s\,m^4}\right)$	1.05e8	$A_d (m^2)$	6.6e-4	$k_{my} \left(\frac{N}{m}\right)$	6.8e4	$z_{m1} (m)$	-0.1348
$R'_i \left(\frac{kg}{m^7}\right)$	4.49e8	$P_0 \left(\frac{N}{m^2}\right)$	10	$k_{mz} \left(\frac{N}{m}\right)$	6.6e4	$z_{m2} (m)$	0.4496
$I_d \left(\frac{kg}{m^4}\right)$	7.5e4	$X_1 (m)$	1e-9	$C_{mx} \left(\frac{N\,s}{m}\right)$	98	$z_{m3} (m)$	-0.4917
$R_d \left(\frac{kg}{s\,m^4}\right)$	1.17e7	$X_2 (m)$	1e-11	$C_{my} \left(\frac{N\,s}{m}\right)$	21		

Appendix B: Vehicle Parameters Values

Table 3. vehicle parameters

Parameter	Amount	Parameter	Amount	Parameter	Amount	Parameter	Amount
$M_e (kg)$	215	$M_{u1}, M_{u4} (kg)$	29.5	$k_{s2}, k_{s3} \left(\frac{N}{m}\right)$	19600	$z'_{m1} (m)$	-0.1348
$I_{ex} (kg\,m^2)$	19	$M_{u2}, M_{u3} (kg)$	27.5	$x'_{m1} (m)$	-0.24	$z'_{m2} (m)$	0.4496
$I_{ey} (kg\,m^2)$	24	$c_{s1}, c_{s4} \left(\frac{N\,s}{m}\right)$	3200	$x'_{m2} (m)$	0.09	$z'_{m3} (m)$	-0.4917
$I_{ez} (kg\,m^2)$	8	$c_{s2}, c_{s3} \left(\frac{N\,s}{m}\right)$	1700	$x'_{m3} (m)$	0	$y_{s1}, y_{s4} (m)$	-1.4
$M_s (kg)$	868	$k_{t1}, k_{t4} \left(\frac{N}{m}\right)$	200000	$y'_{m1} (m)$	-1.31	$y_{s2}, y_{s3} (m)$	1.4
$I_{sy} (kg\,m^2)$	235	$k_{t2}, k_{t3} \left(\frac{N}{m}\right)$	200000	$y'_{m2} (m)$	-1	$z_{s1}, z_{s2} (m)$	-0.72
$I_{sz} (kg\,m^2)$	920	$k_{s1}, k_{s4} \left(\frac{N}{m}\right)$	20580	$y'_{m3} (m)$	-0.91	$z_{s3}, z_{s4} (m)$	0.72